PSFC/JA-15-6

High Field Side Launch of RF Waves: A New Approach to Reactor Actuators

G.M. Wallace, S.G. Baek, P.T. Bonoli, I.C. Faust,
B.L. LaBombard, Y. Lin, R.T. Mumgaard, R.R. Parker,
S. Shiraiwa, R. Vieira, D.G. Whyte and S.J. Wukitch

May, 2015

Plasma Science and Fusion Center
Massachusetts Institute of Technology
Cambridge MA 02139 USA

This work was supported by the U.S. Department of Energy Cooperative Agreement DE-FC02-99ER54512.

High Field Side Launch of RF Waves: A New Approach to Reactor Actuators

G.M. Wallace, S.G. Baek, P.T. Bonoli, I.C. Faust, B.L. LaBombard, Y. Lin, R.T. Mumgaard, R.R. Parker, S. Shiraiwa, R. Vieira, D.G. Whyte and S.J. Wukitch

MIT Plasma Science and Fusion Center, Cambridge, MA 02139 USA

Abstract. Launching radio frequency (RF) waves from the high field side (HFS) of a tokamak offers significant advantages over low field side (LFS) launch with respect to both wave physics and plasma material interactions (PMI). For lower hybrid (LH) waves, the higher magnetic field opens the window between wave accessibility ($n_{||} \equiv ck_{||}/\omega > \sqrt{1-\omega_{pi}^2/\omega^2+\omega_{pe}^2/\omega_{ce}^2}+\omega_{pe}/|\omega_{ce}|$) and the condition for strong electron Landau damping ($n_{||} \sim \sqrt{30/T_e}$ with T_e in keV), allowing LH waves from the HFS to penetrate into the core of a burning plasma, while waves launched from the LFS are restricted to the periphery of the plasma. The lower $n_{||}$ of waves absorbed at higher T_e yields a higher current drive efficiency as well. In the ion cyclotron range of frequencies (ICRF), HFS launch allows for direct access to the mode conversion layer where mode converted waves absorb strongly on thermal electrons and ions, thus avoiding the generation of energetic minority ion tails. The absence of turbulent heat and particle fluxes on the HFS, particularly in double null configuration, makes it the ideal location to minimize PMI damage to the antenna structure. The quiescent SOL also eliminates the need to couple LH waves across a long distance to the separatrix, as the antenna can be located close to plasma without risking damage to the structure. Improved impurity screening on the HFS will help eliminate the long-standing issues of high Z impurity accumulation with ICRF.

Looking toward a fusion reactor, the HFS is the only possible location for a plasma-facing RF antenna that will survive long-term. By integrating the antenna into the blanket module it is possible to improve the tritium breeding ratio compared with an antenna occupying an equatorial port plug. Blanket modules will require remote handling of numerous cooling pipes and electrical connections, and the addition of transmission lines will not substantially increase the level of complexity.

The obvious engineering challenges associated with locating antenna structures on the HFS can be overcome if HFS antennas are incorporated in the overall experimental design from the start. The Advanced Divertor and radio frequency eXperiment(ADX) will include LH and ICRF antennas located on the HFS. Compact antenna designs based on proven technologies (e.g. multi-junction and "4-way splitter" antennas) fit within the available space on the HFS of ADX. Field aligned ICRF antennas are also located on the HFS. The ADX vacuum vessel design includes dedicated space for transmission lines, pressure windows, and vacuum feedthrus for accessing the HFS wall.

Keywords: radio frequency, lower hybrid current drive, ion cyclotron range of frequency, tokamak
PACS: 52.35.Hr, 52.50.Qt, 52.50.Sw, 52.55.Wq

INTRODUCTION

Tokamak reactors will be required to operate with high capacity factor, and therefore very long pulses (i.e. steady state operation) with infrequent maintenance [1]. The limited magnetic flux in the Ohmic transformer requires that non-inductive current drive mechanisms be used for sustaining these steady state discharges. Neutral beams provide a convenient method for generating non-inductive current in present day tokamaks, but neutral beams face major challenges for reactors such as the development of very high energy, steady state beam sources [2], neutron/radiation damage to the source, and negative impact on tritium breeding ratios (TBR). Radio frequency (RF) actuators will likely be needed to fill the gap. Heating and current drive (H&CD) antennas will need to operate continuously for ∼months without failure or maintenance in a tokamak-based power plant. The tokamak power plant will require efficient, off-axis RF heating and current drive actuators to supplement bootstrap current.

Radio frequency H&CD actuators will face extreme challenges in a reactor environment. We have limited experience with a reactor-like environment in regards to plasma material interactions (PMI) and neutron flux. Previous and near-term long-pulse experiments (e.g. TRIAM-1M [3], Tore Supra [4], WEST [5], EAST [6], and ITER [7]) operate in regimes much less severe than reactor. Neutron issues are virtually nonexistent in these long-pulse experiments (except in ITER), and the scrape off layer (SOL) conditions are less likely to produce PMI damage. Concern about the survivability of RF antennas located in close proximity to the low field side (LFS) plasma (LHRF, ICRF, helicon) has

led some to consider these technologies unfit for a reactor environment.

In this paper, we advocate for a different approach to reactor actuators: move H&CD antennas from the low field side to the high field side (HFS) of the tokamak in order to address the issues outlined above. High field side launch experiments have been conducted in the electron cyclotron [8] and ion cyclotron [9] range of frequencies, but not in the lower hybrid range of frequency (LHRF). The benefits of HFS launch in the LHRF were first identified in the Vulcan design study [10], and subsequently applied in the ARC design study [11], but have yet to be tested experimentally. The Advanced Divertor and radio frequency eXperiment (ADX) [12] includes HFS launch LHRF and ICRF and will test both of these technologies in high density, high field conditions envisioned for a reactor.

WAVE PHYSICS BENEFITS

Launching RF waves from the HFS of a tokamak has many advantages in both the lower hybrid range of frequency (LHRF) and the ion cyclotron range of frequency (ICRF).

The propagation and absorption of LH waves are governed in large part by the parallel index of refraction, $n_{||} \equiv ck_{||}/\omega$. Lower hybrid waves damp strongly as $n_{||}$ approaches $\sim \sqrt{30/T_e}$ with T_e in keV [13]. This sets an upper bound on the value of $n_{||}$ that can be used for a discharge with a given temperature. On the other hand, LH waves cannot propagate unless the accessibility condition, $n_{||,acc} > \sqrt{1-\omega_{pi}^2/\omega^2+\omega_{pe}^2/\omega_{ce}^2}+\omega_{pe}/|\omega_{ce}|$, is also satisfied [14]. The meeting of these two inequalities gives rise to the contours in Figure 1(a). The two curves are evaluated using the local magnetic field strength on the LFS and HFS mid-plane at $r/a = 0.7$ for an aspect ratio of 3 and $B_0 = 6.0$ T. The higher field relaxes the accessibility condition, which means that a lower $n_{||}$ can propagate. This allows the wave to penetrate in to a higher temperature at fixed density, or conversely a higher density at fixed temperature. The use of LFS launch LHCD on a fusion reactor with high T_e and n_e pedestals may not be possible, but moving to the HFS increases both the temperature and density to which the LH waves may propagate.

Figure 1(b) shows this benefit from a different view. Here, the accessibility and damping conditions are plotted as a function of normalized minor radius on the HFS and LFS for kinetic profiles of a proposed Fusion Developement Facility (FDF) [15]. The "accessibility window" (shaded region) is clearly larger on the HFS, allowing waves at a lower $n_{||}$ to penetrate deeper into the mid-radius region of the plasma. In addition to the benefits of better wave penetration, the ability to use a lower $n_{||}$ improves current drive efficiency [16]. Ray tracing/Fokker-Planck simulations of FDF indicate a 40% increase in current drive efficiency on the HFS versus LFS, with a broad current profile located near $r/a \sim 0.8$ rather than a narrow profile peaked at $r/a > 0.9$.

High field side launch provides benefits in the ICRF as well. Fast waves launched from the HFS can directly mode convert to ion Bernstein waves (IBW) and ion cyclotron waves (ICW) [17] without tunneling through a cutoff region, which opens the possibility of strong single pass absorption on thermal ions and electrons (rather than creating fast ions). TORIC modeling shows mode converted IBW and ICW with HFS launch, as shown in Figure 2. For $n_H/n_e = 0.15$ (shown in Figure 2), absorption is nearly 100% via mode conversion without generation of fast ions.

Antennas located on the LFS of existing experiments show significant damage after short duration despite relatively hospitable environments of current tokamaks (compared to the heat/neutron fluxes in a reactor). For example, the C-Mod LH antenna shows evidence of PMI damage after short ($t_{pulse} < 0.5$ s) high power pulses in a high heat flux environment on the LFS mid-plane [19], and the JET LHCD system was subjected to significant PMI damage as well [20]. The quiescent HFS SOL is an ideal location for RF antennas. Transport in tokamak geometry sends heat and particles to the bad curvature (i.e. LFS) scrape off layer (SOL). In near double null, the HFS SOL is a private flux region and does not receive the "blobby" transport typical of the LFS SOL. Fluctuation induced particle fluxes are effectively zero on the HFS [21], and edge localized modes (ELMs) also do not reach HFS in double null. The quiescent SOL leads to reduced scattering from density perturbations, which may cause undesirable shifts in the wavenumber spectrum.

High-Z wall materials (e.g. tungsten) will be required in a reactor to avoid tritium co-deposition, but high power RF (particularly ICRF) in a high-Z environment often results in unacceptable impurity content in the plasma. Measurements show that impurity penetration for moderate-Z materials (N_2, CH_4) is 10 times smaller on HFS as compared to the LFS [22, 12], which may reduce the need for low Z (e.g. boron) wall coatings if HFS antennas are used. The HFS also has fewer unconfined fast particles, which have been shown to cause significant damage to in-vessel components. The majority of fast ions (ICRF minority heating and/or fusion-α's) exit on LFS, and runaway electrons also shift their orbits to the LFS. Simulations of ITER lost ion heat loads show peaked heat loads on the LFS with essentially no heat load on the HFS wall [23].

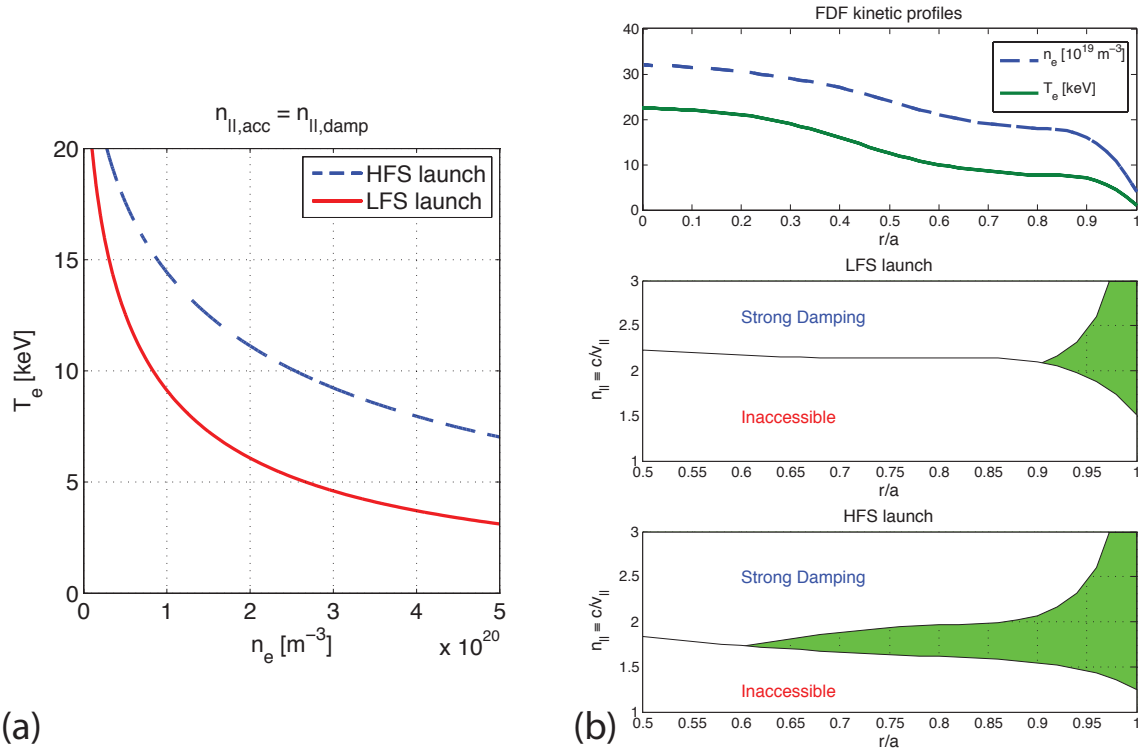

FIGURE 1. (a) Contours of $n_{||,acc} = n_{||,damp}$ for LFS and HFS launch. For a given density, the curves give the approximate maximum temperature to which the LH waves can penetrate, or vice-versa. On-axis magnetic field is 6.0 T for this example. The local magnetic field on the HFS and LFS are evaluated at $r/a = 0.7$. (b) FDF kinetic profiles [15] with accessibility and damping limits plotted on the HFS and LFS mid-plane. The shaded region indicates the window between the two limits. Note the suppressed zero on the abscissa of the bottom two panels.

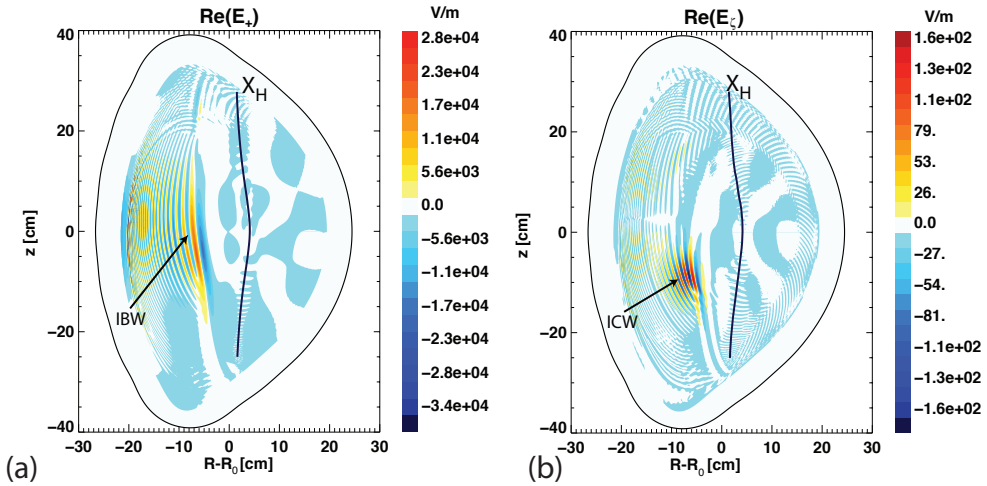

FIGURE 2. (a) Electric field (E_+) calculated for ADX [12] by the TORIC [18] code. The arrow indicates mode conversion to the IBW and subsequent absorption at the ion-ion hybrid resonance layer. The solid line labeled "X_H" indicates the location of the proton cyclotron resonance. (b) Electric field (E_ζ) calculated for ADX by the TORIC code. The arrow indicates mode conversion to the ICW and subsequent absorption at the ion-ion hybrid resonance layer. The solid line labeled "X_H" indicates the location of the proton cyclotron resonance.

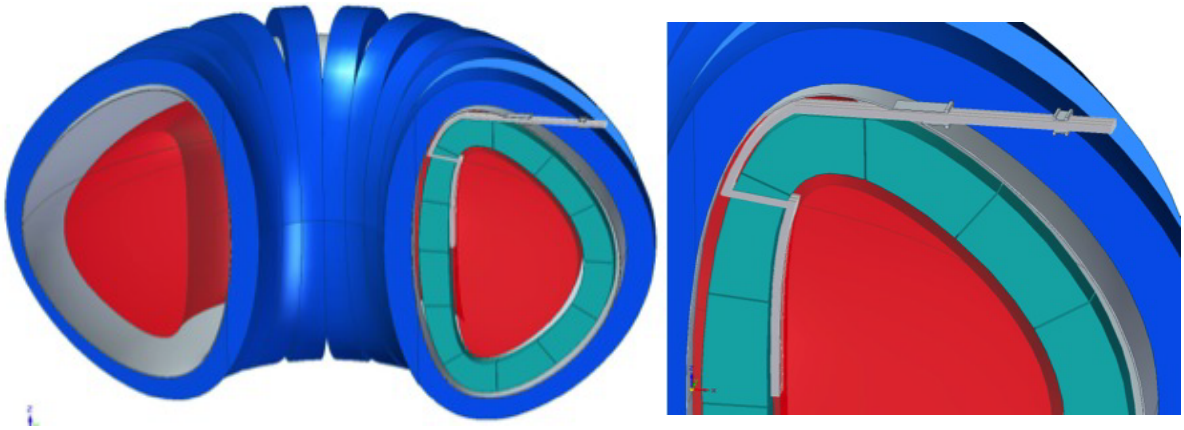

FIGURE 3. Conceptual drawing of compact fusion reactor (∼JET-scale) with HFS antenna integrated into the blanket. Relevant reactor parameters: $R_0 = 3.3$ m, $a = 1.1$ m, $I_p = 6$ MA, $f_{BS} = 0.63$, $I_{LH} = 2.25$ MA, $B_T = 9$ T.

Density and temperature profiles on the HFS are consistent with good coupling from a multi-junction antenna. Although the SOL density profile is steeper on the HFS relative to the LFS, the ability to control precisely the gap between the plasma and the HFS wall, as well as the null balance, allows for control of the density at the LH antenna. Simulations with measured SOL profiles show reflection coefficients of less than 5% across a wide range of edge densities for a compact 4-way multi-junction antenna design.

CONCEPTUAL ENGINEERING ASSESSMENT

In assessing the practicality of HFS antenna systems, it is important not to think in terms of retrofitting to existing tokamak designs. A steady-state tokamak reactor will need to be designed with HFS antennas integrated into the design from the beginning if they are to be practical. The reduced PMI issues on the HFS (discussed in the previous section) will help for the antenna to survive longer without the need for maintenance or replacement. This allows for some trade-off in engineering complexity for the enhanced lifetime of HFS antenna components.

RF system component sizes are roughly set by RF frequency, which in large part is determined by the magnetic field. Space constraints for a reactor relax with larger size, therefore we will consider the smallest possible reactor in the following analysis. A hypothetical JET-scale device with $R_0 = 3.3$ m, $a = 1.1$ m, $I_p = 6$ MA, $f_{BS} = 0.63$, and $I_{LH} = 2.25$ MA is shown in Figure 3. Assuming an efficiency $\eta = 0.3 \times 10^{20}$ AW^{-1}m^{-2}, the tokamak will require $P_{LH} = 40$ MW to provide 2.25 MA of LHCD. Power densities of 40 MW/m^2 power density have been achieved regularly for LHCD antennas at ∼5 GHz, but to be conservative we will multiply the area by a factor of 3 to be conservative and account for passive waveguides, limiters, and the difficulty of long pulse. By this estimate the tokamak will require ∼3 m^2 of area for the radiating surface. In constrast, the area of the center stack is ∼54 m^2. A mostly toroidally continuous antenna (accounting for "bumper" limiters every ∼20 columns) would only need to be 0.3 m high (∼4 rows of waveguides at 5 GHz).

A compact multi-junction [24] antenna design for HFS use is shown in Figure 4. The multi-junction is designed to fit within the envelope of a WR187 waveguide (standard size fundamental waveguide at 4.6 GHz for a single output row. The waveguide is intended to run up (or down) the HFS wall between the plasma facing armor and the breeding material to the desired poloidal launch point, and requires only ∼ 5 cm of space in the radial dimension. Figure 3 shows a possible waveguide feed route for a HFS antennas in a "JET-scale" reactor. A pair of windows are located outside the toroidal field (TF) coils to prevent an accidental release of tritium in case one window fails. A tertiary vacuum window may be located inside the TF coil where the waveguide pierces the vacuum vessel. This would allow for pressurization in the region where $\omega_0 = \omega_{ce}$ as the waveguide passes through the TF coil. The waveguide then runs inside the vacuum vessel to near the upper divertor, where it passes through the blanket module towards the plasma facing components, then finally down the inner wall to radiating apertures at the desired poloidal launch point. The location of the penetration through the blanket module is at a minimum of the neutron wall loading to minimize the impact of the hole through the blanket on both tritium breeding and component shielding.

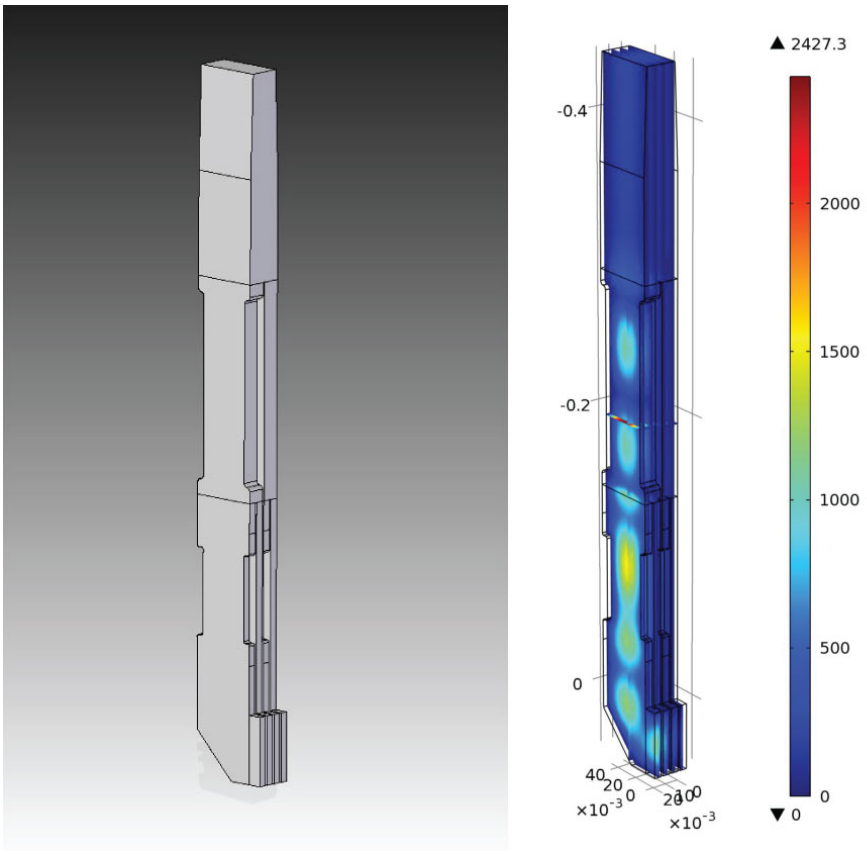

FIGURE 4. A compact 4-way multi-junction design for HFS launch. The input waveguide at the top is conventional WR187 for 4.6 GHz. The first split introduces a (0°, 180°) phase shift. The second pair of splitters introduce a (0°, 90°) phase shift for an overall phase output of (0°, 90°, 180°, 270°) at the radiating apertures. The radiating apertures are 5.5 mm × 60 mm in dimension with a 1.5 mm septum. The right plot shows simulated $|\vec{E}|$ in the splitter assembly.

Studies of neutron wall loading in reactors [25, 26] show that the HFS has lower neutron wall loading than LFS midplane, and the HFS blanket contributes less to TBR than the LFS blanket even when accounting for the difference in surface area between the HFS and LFS. A radial port plug on LFS gives large line-of-sight (LOS) through breeding blanket and "channels" neutrons down the port. However, a HFS antenna integrated into the blanket module has less significant LOS given that it is in a low neutron flux region. The thickness of a HFS blanket module could increase slightly (5-10 cm) to compensate for void of waveguide between the plasma facing armor and the breeding material, although some blanket designs such as those for the recent ARIES-ACT1 and ACT2 studies [27] already include a similarly sized void between the plasma facing surface and the breeding material. The ARIES-ACT1 blanket design includes inner and outer interlocking "C" shaped blanket modules with a radial gap between the blankets for divertor pumping. This design lends itself well to routing RF transmission lines to the HFS. Waveguides (or rigid coaxial cable) could pass through a similar sized gap between the LFS and HFS blankets, above the upper (or below the lower) divertor modules, and then vertically along the HFS wall between the breeding material and the plasma facing armor.

High field side antennas will no doubt be difficult to replace without removing the associated blanket modules; therefore, antennas should be designed to last for the lifetime of the blanket module and replaced when you replace first wall tiles and/or blanket module. The less extreme conditions of the HFS SOL (as compared to the LFS SOL) should lead to less maintenance required for HFS antennas. The lower PMI and neutron flux will extend the lifespan of materials on HFS, and the use of resilient materials with new techniques (e.g. 3D printing of Tungsten) for HFS antenna components will increase longevity further. This should allow for replacement or repair of HFS antennas on a similar schedule as the other invessel components.

Three leading concepts for reactor maintenance are all compatible with HFS RF antennas. The segmented blanket

concept (illustrated in Figure 3), as incorporated into the ITER design and proposed for other DEMO type devices, already has many connections for cooling, tritium, diagnostics behind each of the complicated breeding blanket modules. Each of these connections must be made by remote handling (i.e. robotic arm) due to high activation levels within the vacuum vessel. Adding a waveguide connection to a subset of the blanket modules will not significantly add to the complexity of the remote handling problem in this concept.

The ARIES-ACT1 study uses a sector maintenance concept [28] to replace complete wedge-shaped sectors of the blanket and first wall as integrated units. In this maintenance scheme the HFS antennas would be integrated into the sector and removed/replaced with the rest of the first wall and blanket components.

The vertical lift maintenance scheme included in the ARC study [11] consists of a vacuum vessel/first wall assembly immersed in a liquid breeding material tank. The entire vacuum vessel, along with associated invessel components, are designed to be removed vertically and replaced as a unit through the use of demountable toroidal field coils. The ARC design study includes HFS antennas built into vacuum vessel, to be replaced at same time as the vessel.

The Advanced Divertor and radio frequency eXperiment (ADX) [12], a facility proposed by the MIT PSFC and collaborators from a wide range of institutions, is designed to verify the benefits of HFS launch described above. The design includes demountable toroidal field coils along with a set of flexible divertor coils. The high field ($B_0 \leq 8$ T), electron density ($\bar{n}_e = 0.5 - 2.5 \times 10^{20}$ m^{-3}), RF power density (~ 10 MWm^{-3}), and high-Z wall material (tungsten and/or molybdenum) make ADX an ideal test bed for HFS launch of RF waves. The flexible divertor coils allow for exploration of advanced divertor concepts (super-x, x-point target, snowflake, etc) including compatibility with RF actuators.

Inner wall RF antennas in the LHRF and ICRF are included in the design. Figure 5 shows computer renderings of the ADX design including HFS ICRF and LHRF antennas. Both antenna designs are fed by transmission lines that traverse above (below) the upper (lower) divertor before running along the HFS wall to the desired launch point. The HFS LHRF antenna shown in the rendering is based on the 4 way poloidal splitter concept used in the "LH2" launcher on C-Mod combined with a toroidal 90° bi-junction to split each input waveguide into 8 radiating apertures. The feed waveguide transits radially above the upper divertor, passes through the vacuum vessel, then turns 90° down along the HFS wall to the radiating apertures at and below the plasma mid-plane. The splitters are grouped into discrete launchers consisting of 4 feed waveguides dividing into an 8 column $\times$ 4 row phased array with the launchers separated toroidally by a bumper limiter to protect against damaged during startup/rampdown and disruptions. An HFS ICRF antenna is also included in the design. The HFS ICRF antenna is fed at both ends by coaxial transmission lines, which transition to shielded striplines at the top and bottom of the inner wall. The center of the strap is grounded to the wall.

CONCLUSIONS

HFS launch can improve H&CD performance, antenna longevity, and reduce the negative impact of RF antennas on tritium breeding, in addition to benefits for wave propagation and absorption physics in both the ICRF and LHRF. Launching LH waves at lower $n_{||}$, possible thanks to the higher magnetic field, leads to higher current drive efficiency and better wave penetration through the pedestal in a reactor. Launching the ICRF fast wave gives direct access to ICW/IBW mode conversion layer and opens the door for efficient absorption on thermal ions and electrons. The quiescent HFS SOL has lower heat and particle fluxes, particularly in double null, will extend antenna longevity. Strong impurity screening will also mitigate the effect of impurity generation by RF antennas located on the HFS.

Conceptual engineering assessments for HFS RF antennas look feasible. Real estate on the HFS is less critical for tritium breeding due to lower neutron fluxes, and sufficient surface area exists for antennas to be installed assuming conservative power densities. High field side RF antennas are possible to implement, but the tokamak must be designed with HFS antennas as an initial constraint, rather than as a retrofit. Remote maintenance concepts proposed for tokamak reactors are compatible with HFS RF antennas. Detailed designs for the ADX facility include HFS ICRF and LHRF antennas to test experimentally the benefits of HFS launch for RF actuators.

ACKNOWLEDGMENTS

The authors would like to thank Rick Leccacorvi (MIT PSFC) for his assistance with creating CAD drawings for this paper, and Chuck Kessel (PPPL) for helpful discussions on the implications of HFS launch for reactors. This work supported by US Department of Energy cooperative agreement DE-FC02-99ER54512.

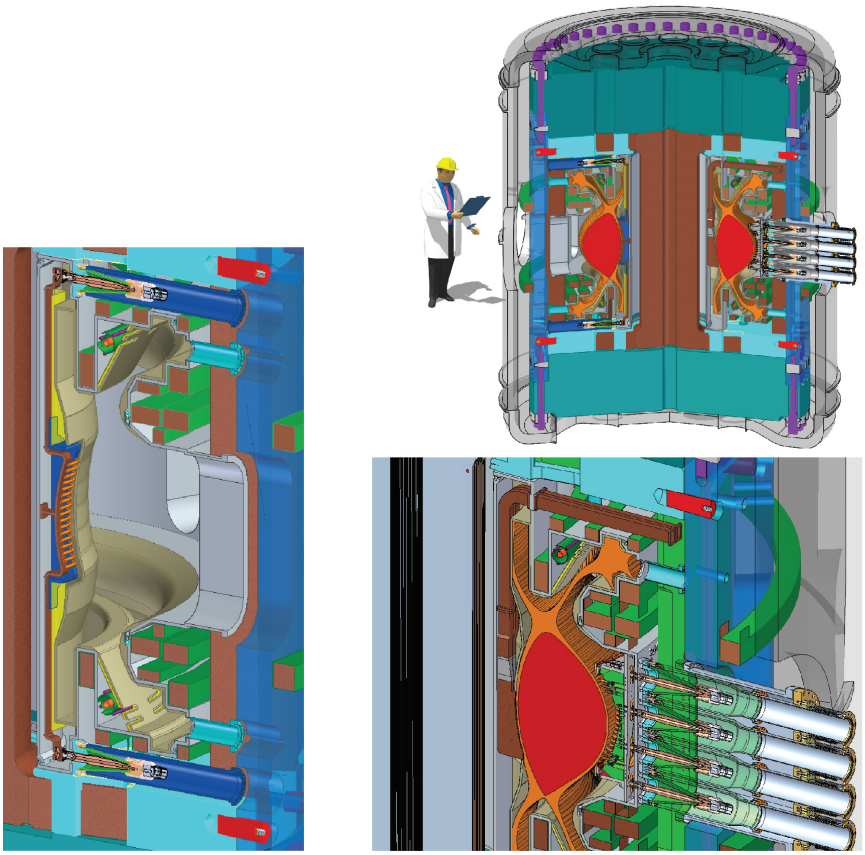

FIGURE 5. (top right) Computer rending of the complete ADX assembly with person for scale. (bottom right) Detail view of ADX HFS LHRF antenna. The feed waveguide transits radially above the upper divertor, passes through the vacuum vessel, then turns 90° down along the HFS wall to the radiating apertures below the plasma mid-plane. A LFS ICRF antenna is also included in the design for comparison between HFS and LFS launch points. (left) Detailed view of ADX HFS ICRF antenna. The antenna is fed at both ends by coaxial transmission lines, which transition to shielded striplines at the top and bottom of the inner wall. The center of the strap is grounded to the wall.

REFERENCES

1. T. C. Luce, *Physics of Plasmas (1994-present)* **18**, – (2011), URL http://scitation.aip.org/content/aip/journal/pop/18/3/10.1063/1.3551571.
2. U. Fantz, P. Franzen, and D. Wuenderlich, *Chemical Physics* **398**, 7 – 16 (2012), ISSN 0301-0104, URL http://www.sciencedirect.com/science/article/pii/S0301010411001601, chemical Physics of Low-Temperature Plasmas (in honour of Prof Mario Capitelli).
3. H. Zushi, S. Itoh, K. Hanada, K. Nakamura, M. Sakamoto, E. Jotaki, M. Hasegawa, Y. Pan, S. Kulkarni, A. Iyomasa, S. Kawasaki, H. Nakashima, N. Yoshida, K. Tokunaga, T. Fujiwara, M. Miyamoto, H. Nakano, M. Yuno, A. Murakami, S. Nakamura, N. Sakamoto, K. Shinoda, S. Yamazoe, H. Akanishi, K. Kuramoto, Y. Matsuo, A. Iwamae, T. Fuijimoto, A. Komori, T. Morisaki, H. Suzuki, S. Masuzaki, Y. Hirooka, Y. Nakashima, and O. Mitarai, *Nuclear Fusion* **43**, 1600 (2003), URL http://stacks.iop.org/0029-5515/43/i=12/a=006.
4. Y. Peysson, and T. S. Team, *Nuclear Fusion* **41**, 1703 (2001), URL http://stacks.iop.org/0029-5515/41/i=11/a=320.
5. A. Grosman, J. Bucalossi, L. Doceul, F. Escourbiac, M. Lipa, M. Merola, M. Missirlian, R. A. Pitts, F. Samaille, and E. Tsitrone, *Fusion Engineering and Design* **88**, 497 – 500 (2013), ISSN 0920-3796, URL http://www.sciencedirect.com/science/article/pii/S0920379613001531, proceedings of the 27th Symposium On Fusion Technology (SOFT-27); LiÃĺge, Belgium, September 24-28, 2012.
6. L. Zhao, J. Shan, F. Liu, H. Jia, M. Wang, L. Liu, X. Wang, and H. Xu, *Plasma Science and Technology* **12**, 118 (2010), URL http://stacks.iop.org/1009-0630/12/i=1/a=25.
7. G. Hoang, A. Bécoulet, J. Jacquinot, J. Artaud, Y. Bae, B. Beaumont, J. Belo, G. Berger-By, J. P. Bizarro, P. Bonoli, M. Cho, J. Decker, L. Delpech, A. Ekedahl, J. Garcia, G. Giruzzi, M. Goniche, C. Gormezano, D. Guilhem, J. Hillairet, F. Imbeaux,

F. Kazarian, C. Kessel, S. Kim, J. Kwak, J. Jeong, J. Lister, X. Litaudon, R. Magne, S. Milora, F. Mirizzi, W. Namkung, J. Noterdaeme, S. Park, R. Parker, Y. Peysson, D. Rasmussen, P. Sharma, M. Schneider, E. Synakowski, A. Tanga, A. Tuccillo, and Y. Wan, *Nuclear Fusion* **49**, 075001 (2009), URL http://stacks.iop.org/0029-5515/49/i=7/a=075001.
8. T. C. Luce, et al., *Proceedings of the 13th Int. Conf. on Plasma Phys. and Control. Nuclear Fusion Res.* **3**, 631 (1990).
9. Equipe TFR, *Plasma Physics* **24**, 615 (1982), URL http://stacks.iop.org/0032-1028/24/i=6/a=004.
10. Y. Podpaly, G. Olynyk, M. Garrett, P. Bonoli, and D. Whyte, *Fusion Engineering and Design* **87**, 215 – 223 (2012), ISSN 0920-3796, URL http://www.sciencedirect.com/science/article/pii/S0920379611006314.
11. B. Sorbom, J. Ball, T. Palmer, F. Mangiarotti, J. Sierchio, P. Bonoli, C. Kasten, D. Sutherland, H. Barnard, C. Haakonsen, J. Goh, C. Sung, and D. Whyte, ARC: A compact, high-field, fusion nuclear science facility and demonstration power plant with demountable magnets (2014), submitted for publication in *Fusion Engineering and Design*.
12. B. LaBombard, E. Marmar, J. Irby, J. Terry, R. Vieira, G. Wallace, D. Whyte, S. Wolfe, S. Wukitch, S. Baek, W. Beck, P. Bonoli, D. Brunner, J. Doody, R. Ellis, D. Ernst, C. Fiore, J. Freidberg, T. Golfinopoulos, R. Granetz, M. Greenwald, Z. Hartwig, A. Hubbard, J. Hughes, I. Hutchinson, C. Kessel, M. Kotschenreuther, R. Leccacorvi, Y. Lin, B. Lipschultz, S. Mahajan, J. Minervini, R. Mumgaard, R. Nygren, R. Parker, F. Poli, M. Porkolab, M. Reinke, J. Rice, T. Rognlien, W. Rowan, S. Shiraiwa, D. Terry, C. Theiler, P. Titus, M. Umansky, P. Valanju, J. Walk, A. White, J. Wilson, G. Wright, and S. Zweben, *Nuclear Fusion* **55**, 053020 (2015), URL http://stacks.iop.org/0029-5515/55/i=5/a=053020.
13. P. T. Bonoli, and R. C. Englade, *Physics of Fluids* **29**, 2937–2950 (1986).
14. V. E. Golant, *Soviet Physics Technical Physics* **16**, 1980 (1972).
15. V. S. Chan, R. D. Stambaugh, A. M. Garofalo, M. S. Chu, R. K. Fisher, C. M. Greenfield, D. A. Humphreys, L. L. Lao, J. A. Leuer, T. W. Petrie, R. Prater, G. M. Staebler, P. B. Snyder, H. E. S. John, A. D. Turnbull, C. P. C. Wong, and M. A. V. Zeeland, *Fusion Science and Technology* **57**, 66–93 (2010).
16. N. J. Fisch, *Reviews of Modern Physics* **59**, 175–234 (1987).
17. E. Nelson-Melby, M. Porkolab, P. T. Bonoli, Y. Lin, A. Mazurenko, and S. J. Wukitch, *Phys. Rev. Lett.* **90**, 155004 (2003), URL http://link.aps.org/doi/10.1103/PhysRevLett.90.155004.
18. M. Brambilla, A full wave code for ion cyclotron waves in toroidal plasmas, Tech. rep., Max-Planck-Institut für Plasmaphysik, Garching (Germany) (1996).
19. G. M. Wallace, *Behavior of Lower Hybrid Waves in the Scrape Layer of a Diverted Tokamak*, Ph.D. thesis, Massachusetts Institute of Technology (2009).
20. K. K. Kirov, J. Mailloux, A. Ekedahl, and L. team JET EFDA Contributors, *RADIO FREQUENCY POWER IN PLASMAS: 16th Topical Conference on Radio Frequency Power in Plasmas* **787**, 315–318 (2005).
21. N. Smick, B. LaBombard, and I. Hutchinson, *Nuclear Fusion* **53**, 023001 (2013), URL http://stacks.iop.org/0029-5515/53/i=2/a=023001.
22. G. McCracken, R. Granetz, B. Lipschultz, B. Labombard, F. Bombarda, J. Goetz, S. Lisgo, D. Jablonski, H. Ohkawa, J. Rice, P. Stangeby, J. Terry, and Y. Wang, *Journal of Nuclear Materials* **241 - 243**, 777 – 781 (1997), ISSN 0022-3115, URL http://www.sciencedirect.com/science/article/pii/S0022311597801390.
23. K. Shinohara, T. Kurki-Suonio, D. Spong, O. Asunta, K. Tani, E. Strumberger, S. Briguglio, T. Koskela, G. Vlad, S. GÃijnter, G. Kramer, S. Putvinski, K. Hamamatsu, and I. T. G. on Energetic Particles, *Nuclear Fusion* **51**, 063028 (2011), URL http://stacks.iop.org/0029-5515/51/i=6/a=063028.
24. C. Gormezano, P. Briand, G. Briffod, G. Hoang, T. N'Guyen, D. Moreau, and G. Ray, *Nuclear Fusion* **25**, 419 (1985), URL http://stacks.iop.org/0029-5515/25/i=4/a=002.
25. L. Packer, R. Pampin, and S. Zheng, *Journal of Nuclear Materials* **417**, 718 – 722 (2011), ISSN 0022-3115, URL http://www.sciencedirect.com/science/article/pii/S0022311510009475, proceedings of ICFRM-14.
26. M. Z. Youssef, R. Feder, and I. M. Davis, *Fusion Engineering and Design* **83**, 1661 – 1668 (2008), ISSN 0920-3796, URL http://www.sciencedirect.com/science/article/pii/S0920379608001336, proceedings of the Eigth International Symposium of Fusion Nuclear Technology ISFNT-8 {SI}.
27. C. E. Kessel, M. S. Tillack, F. Najmabadi, F. M. Poli, K. Ghantous, N. Gorelenkov, X. R. Wang, D. Navaei, H. H. Toudeshki, C. Koehly, L. EL-Guebaly, J. P. Blanchard, C. J. Martin, L. Mynsburge, P. Humrickhouse, M. E. Rensink, T. D. Rognlien, M. Yoda, S. I. Abdel-Khalik, M. D. Hageman, B. H. Mills, J. D. Rader, D. L. Sadowski, P. B. Snyder, H. S. John, A. D. Turnbull, L. M. Waganer, S. Malang, and A. F. Rowcliffe, *Fusion Science and Technology* **67**, 1–21 (2015), URL dx.doi.org/10.13182/FST14-794.
28. X. R. Wang, M. S. Tillack, C. Koehly, S. Malang, H. H. Toudeshki, F. Najmabadi, and the ARIES Team, *Fusion Science and Technology* **67**, 22–48 (2015), URL dx.doi.org/10.13182/FST14-797.